Available online at **www.joac.info**

ISSN: 2278-1862

Journal of Applicable Chemistry

2020, 9 (4): 547-555

(International Peer Reviewed Journal)

Green Synthesis of Nickel oxide Nanoparticles using *Acalypha Indica* Leaf Extract, Characterization and Study of its Photocatalytic Activity

Hosaholalu Balakrishna Uma and Sannaiah Ananda*

Department of Studies in Chemistry, Manasagangotri, University of Mysore, Mysuru-570006, **INDIA**

Email: snananda@yahoo.com

Accepted on 7th July, 2020

ABSTRACT

Green protocol for the synthesis of nickel oxide nanoparticles has been employed as it is rapid, eco-friendly and cost-effective and better than chemical synthetic methods. The nickel oxide nanoparticles were synthesized by green routes using the leaf extract of Acalypha Indica plant. The obtained nanoparticles were characterized by XRD, FE-SEM, UV-Visible and FT-IR techniques. The average crystallite size of the nanoparticles calculated from Debye Scherrer equation using XRD data was found to be 68.3 nm with FCC structure. The maximum absorption of the NiO nanoparticles is 346 nm and band gap calculated from Tauc's plot was found to be 2.95 eV. The photocatalytic activity of prepared nanoparticles was studied by the degradation of textile dye indigo carmine under ultraviolet radiation. The COD measurements were carried out to study the catalytic efficiency of the nanoparticles.

Graphical Abstract

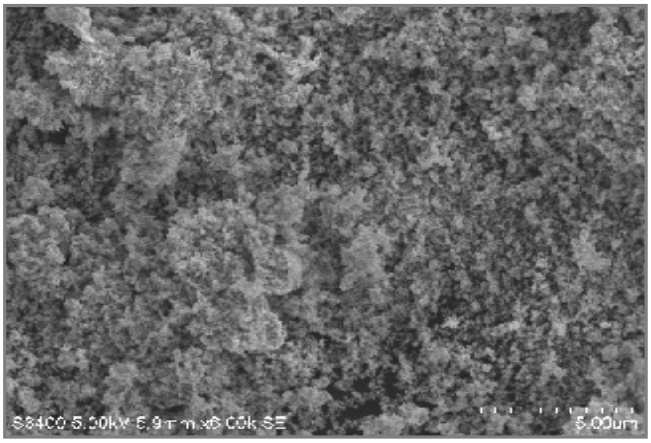

SEM image of NiO nanoparticles.

Keywords: *Acalypha Indica*, NiO nanoparticles, Photodegradation.

INTRODUCTION

Transition metal oxide nanoparticles find their application as sensors, catalysts, batteries, ceramics, small energy efficient materials and electronic applications. Transition metal oxides like nickel oxide has becoming one of the most important nanomaterial because of its outstanding catalytic property, electrical application and fuel cell electrode preparations [**1-3**]. NiO is a p-type semiconductor with wide band gap of 3.6-4.0 eV and known for its better qualities and applications such as photocatalytic, sensors, magnetic resonance imaging, memory storage devices. NiO is well known for its applications in medicinal field which includes the production of hygiene products, cosmetics, antibiotics, nanocarriers for the purpose of transferring and releasing drugs at the targeted cells along with their growing trend in the imaging of cells and treatment of cancer [**4**]. Numerous methods for the synthesis of NiO nanoparticles have been reported in the literature which includes sol-gel method, co-precipitation, electrode deposition, sputtering, thermal decomposition, spray pyrolysis, polymer-matrix assisted synthesis, ultrasonic radiation, hydrothermal synthesis, laser chemical method, pyrolysis by microwave, micro-emulsion, combustion method, surfactant mediated synthesis and precipitation-calcination methods [**5-16**]. These physical and chemical methods may have low productivity, high cytotoxicity, low antioxidant property, low antibacterial activity and may not be eco-friendly [**17**]. However in the recent years there is great concern from researchers to search for environmentally friendly methods for the synthesis of nanomaterials which results in the development of bionanotechnology. In bionanotechnology, the nanopaticles are synthesized by using biological systems which includes plants, bacteria, fungi, yeast and naturally occurring tiny molecules such as proteins, vitamins, peptides and reducing sugars [**18**]. The combination of biological principles i.e. oxidation/reduction with plant phytochemicals with desired physical and chemical approaches results in the synthesis of nanoparticles with desired properties and functions. Biosynthesis provides a simple, inexpensive and environmentally friendly approach for the synthesis of nanomaterials which have no or low cytotoxicity compared to the chemically synthesized nanomaterials which makes them efficient carriers of drugs for in vivo drug delivery applications [**19-21**].

In this present work, the green synthesis of NiO nanoparticles using *Acalypha Indica* leaf extract has been reported. The composition, structural and optical properties were studied by EDAX, FE-SEM, XRD, FT-IR and UV-Visible characterization of the nanoparticles. The photocatalytic activity of the synthesized NiO nanoparticles were studied using indigo carmine dye under UV radiation and degradation efficiency has been reported.

.

MATERIALS AND METHODS

Nickel sulphate supplied by alfa-aesar was used for synthesis. Deionized water was used for all experiments. All chemicals were used as received without further purification.

Collection of plant materials and preparation of plant extract: The *Acalypha Indica*leaves were collected washed well with water and shade dried up to ten days. After dried, leaves were made into fine powder by mechanical grinding and sieved. The fine powder thus obtained was used for the preparation of the extract. About 50 g of pure, dried and powdered *Acalypha Indica* was taken in 500 mL beaker and 300 mL of methanol was added and mixed well. The solution was stirred using magnetic stirrer for 24 h for complete extraction of all the organic components present in it and then filtered using Whattman No.41 filter paper. The filtrate then heated gently for evaporation of methanol and 150 mL of distilled water was added to get the plant extract.

Biosynthesis of NiO nanoparticles using leaf extract: About of 50 mL of *AcalyphaIndica* leaf extract was taken in a beaker and 50 mL of 0.1 M nickel sulphate was added dropwise with constant stirring at ambient temperature. The reaction mixture was then centrifuged and the obtained NiO nanoparticles were washed repeatedly with distilled water to remove unbound phyto constituents. The

nanoparticles were then calcined at 600°C in muffle furnace. The black colored NiO nanoparticles thus obtained were collected and used for further characterization.

Characterization techniques: The XRD pattern of NiO nanoparticles was recorded using Rigaku Miniflex II desktop X-ray diffractometer equipped with Cu-Kα radiation (λ = 0.1540 nm). The SEM images of the sample were recorded on ESEM Quanta-200 FEI- Netherlands. The optical absorption spectra was measured in the wavelength range 200-800 nm using JASCO UV-Vis spectrophotometer. The FT-IR measurements were performed using JASCO, FT-IR in the spectral range of 4000-500 cm^{-1}.

RESULTS AND DISCUSSION

X-ray diffraction (XRD): The XRD pattern of NiO nanoparticles is displayed in the figure 1 which exhibits sharp diffraction peaks. The (hkl) values of the peaks 37.26°, 43.30°, 62.88°, 75.42° and 79.37° corresponds to the crystal planes of (111), (200), (220), (311) and (222) respectively. The average crystallite size calculated using Debye Scherrer equation was found to be 68.3 nm. The crystal structure parameters a = b = c = 4.177 Å, and α = β = γ = 90°. Accordingly, NiO belongs to face centered cubic crystal system. The obtained diffraction peaks are well in agreement with that of the reported XRD results (JCPDS file no. 04-0835)[**15, 16, 22**].

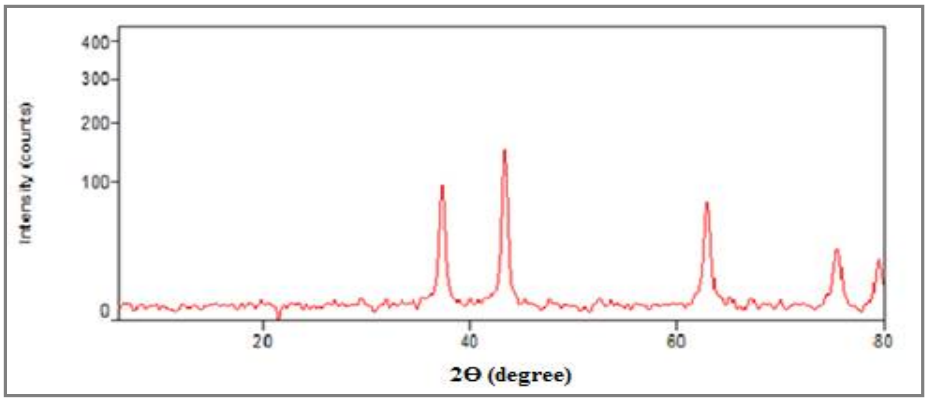

Figure 1. XRD of NiO nanoparticles.

Fourier Transform Infrared analysis (FT-IR): FT-IR spectrum of the NiO nanoparticles is showed in figure 2. In general, the FT-IR bands occur due to metal-oxygen occurs in the region between 400-850 cm^{-1}. The band at 618 cm^{-1} is associated with Ni-O-H stretching bond [**23**].

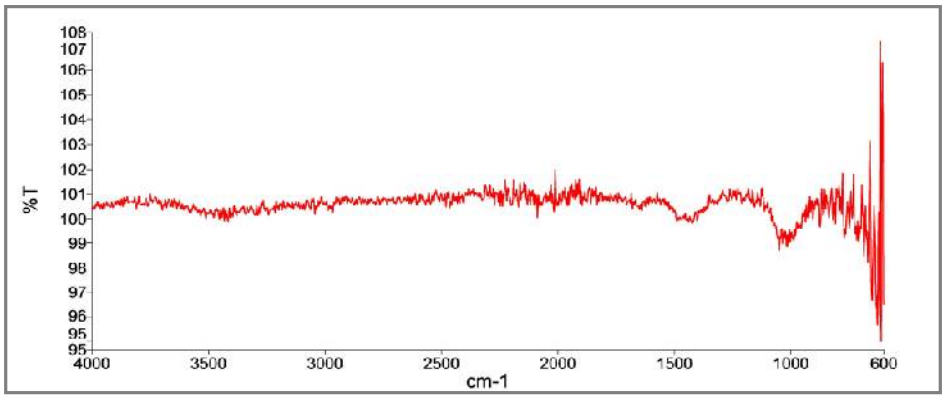

Figure 2. FT-IR spectrum of NiO nanoparticles.

Ultraviolet-Visible spectroscopy: From the optical absorption spectrum indicated by figure 3, it is clear that the maximum absorption for NiO nanoparticles is at 346 nm. This peak reflects the band gap of the nanoparticles and the synthesized nanoparticles are photoactive under UV light. There is no absorption peak in the visible region. The band gap of the sample is calculated using Tauc's plot [**24, 25**] by plotting $(\alpha h\nu)^{1/2}$ verses hν and then extrapolating the straight portion of the curve on hν axis and it found to be 2.95 eV which is lower than that of the bulk NiO (Eg= 3.74eV) represented by figure 4 [**4, 26**].

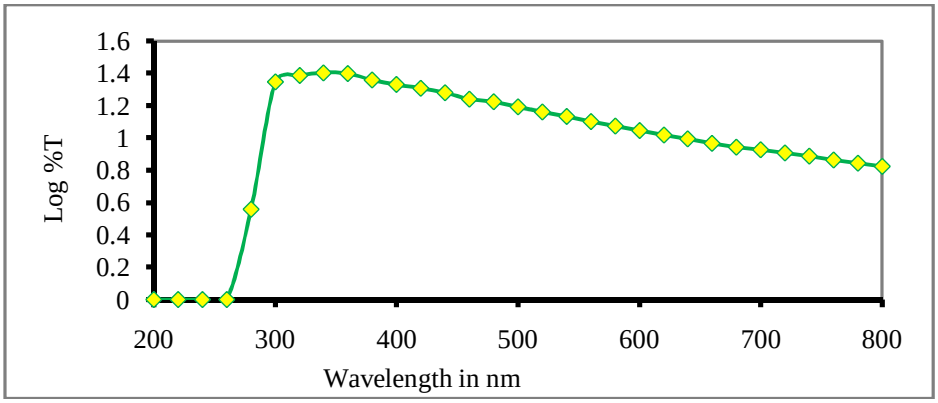

Figure 3. UV-Visible spectrum of NiO nanoparticles.

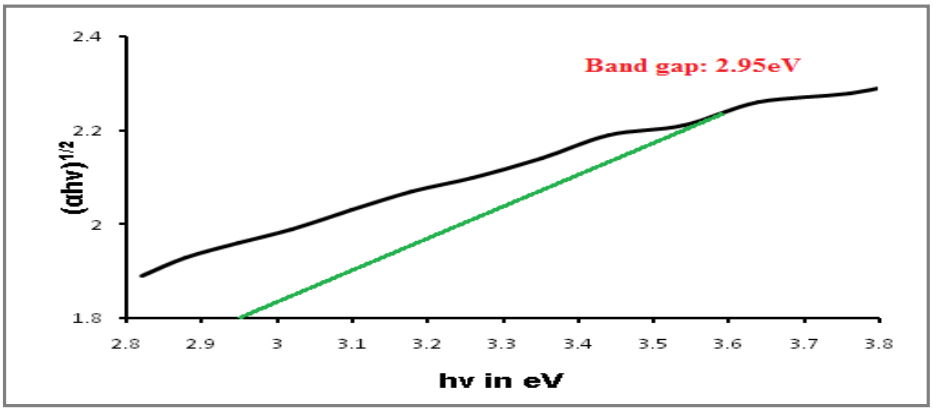

Figure 4. Tauc's plot of NiO nanoparticles.

Energy dispersive X-ray analysis (EDAX) The EDAX confirmed the presence of constituent elements Ni and O without any impurity represented by figure 5.

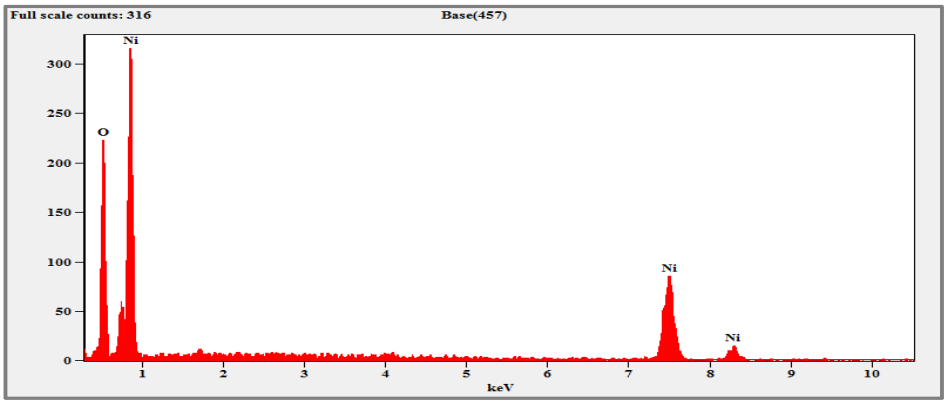

Figure 5. EDAX of NiO nanoparticles.

Scanning electron microscopy (SEM): The morphology of the NiO nanoparticles investigated by SEM represented by figure 6 suggests that the sample consists of agglomerated particles.

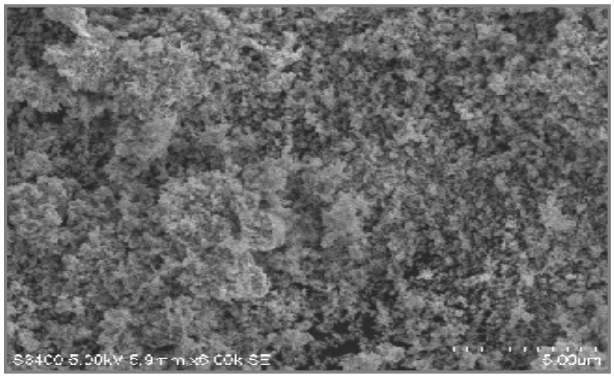

Figure 6. SEM of NiO nanoparticles.

APPLICATION

Mineralization of indigo carmine dye: The photocatalytic property of the prepared NiO nanoparticles were assessed by the degradation of indigo carmine dye under UV irradiation. The photodegradation experiments were carried out using different concentration of indigo carmine dye as substrate and different amounts of NiO as catalyst. A calculated quantity of nanoparticles was added to the dye solution, stirred in dark for 1 minute to establish adsorption/desorption equilibrium between the dye and nanoparticle molecules and the illuminated under UV source to induce a photochemical reaction. The % T was determined by Elico SL 171 mini spectrometer for aliquots taken at an interval of 10 min. Chemical oxygen demand was measured according to standard dichromate titration method. Adsorption and photocatalytic conversion (g %) was calculated. The decrease in COD of the solution gives the measure of mineralization of the dye solution.

Effect of catalyst loading: Table 1 shows the rate of photodegradation of indigo carmine at different concentrations of NiO catalyst. The photocatalytic rate initially higher and then decreases with catalyst loading due to light scattering and screening effects [27]. The tendency towards agglomeration also increases at higher concentration, resulting in a reduction in the surface area available for light absorption and a decrease in photo catalytic rate. The number of active sites in the solution will increase with catalyst loading, a point appears to be reached where light penetration is compromised because of excessive particle concentration (Figure 7). A further increase in catalyst loading beyond the optimum will result in non linear light intensity distribution, so that the reaction rate would indeed be lower with increased catalyst loading [28].

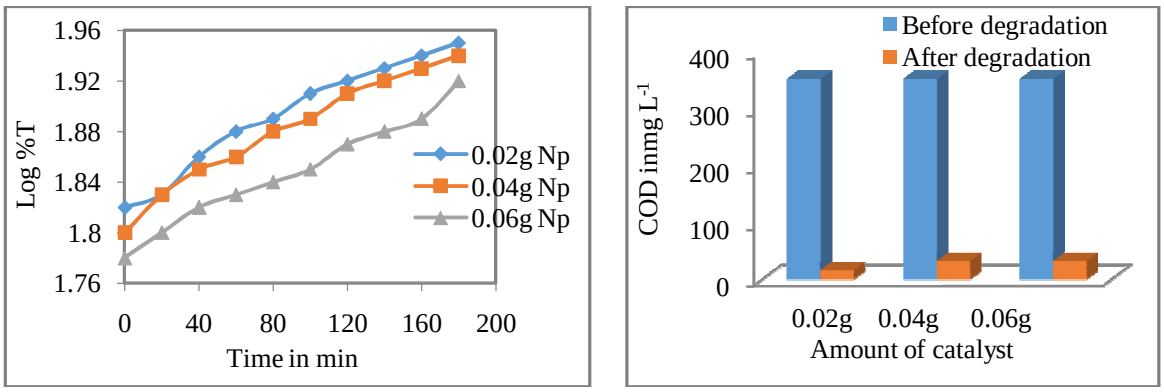

Figure 7. Plot of log % T Vs time with respect to catalyst loading and COD values upon degradation.

Table 1. Effect of catalyst loading on the rate of photodegradation

Variation	Amount of catalyst	k in sec^{-1}	COD values in mg L^{-1}		Degradation efficiency (%)
			Before degradation	After degradation	
Amount of catalyst	0.02g	3.27×10^{-5}	352	16	95.45
	0.04g	2.68×10^{-5}	352	32	90.90
	0.06g	2.65×10^{-5}	352	32	90.90

Effect of concentration of dye: The effect of concentration of indigo carmine dye on photodegradation was studied with constant weight of catalyst. The rate of indigo carmine decolorization initially increased and then decreased markedly with increasing concentration of the dye. The possible reason is that with increase in concentration of dye, the solution becomes more intense colored and path length of the photons entering the solution is decreased and hence fewer photons will reach the catalyst surface. Also, as the initial concentration of dye increased, more dye molecules are adsorbed onto the catalyst surface and decreases the degradation efficiency [27]. Hence there will be a reduction in the production of hydroxyl and superoxide radicals [29]. This is due to limited surface area and active sites of the catalyst. Since the amount of catalyst and intensity of light are constant, the adsorbed dye molecules are not degraded immediately and decrease the efficiency [30] (Figure 8).

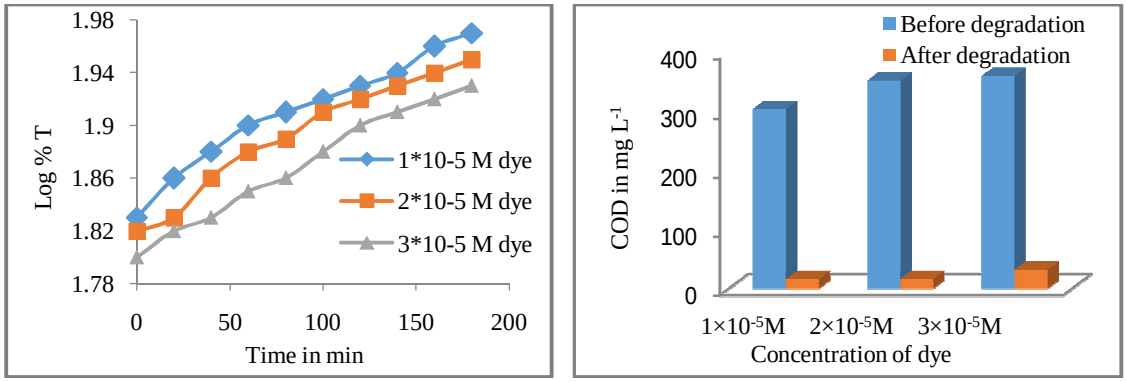

Figure 8. Plot of log % T Vs time with respect to different initial concentration of dye and COD values.

Table 2. Effect of concentration of dye on the rate of degradation

Variation	Concentration of dye	k in sec^{-1}	COD values in mg L^{-1}		Degradation efficiency (%)
			Before degradation	After degradation	
Concentration of dye	1×10^{-5}M	3.59×10^{-5}	304	16	94.73
	2×10^{-5}M	3.27×10^{-5}	352	16	95.45
	3×10^{-5}M	2.87×10^{-5}	360	32	91.11

Re-use of catalyst: The photocatalyst was thoroughly washed with double distilled water, dried and reused for photodegradation by taking a fresh sample of indigo carmine dye solution. A slight decrease in the rate of reaction and loss of catalytic activity was observed with the second use of catalyst (Figure 9). The fresh sample of nano NiO catalyst showed 95.45 % efficiency while the reused sample shown 82.82 % efficiency (Table 3).

Table 3. Efficiency of catalyst for second use

Variation	Concentration of dye	k in sec^{-1}	COD values in mg L^{-1}		Degradation efficiency (%)
			Before Degradation	After Degradation	
Re-use of catalyst	2×10^{-5}M	2.55×10^{-5}	360	64	82.82

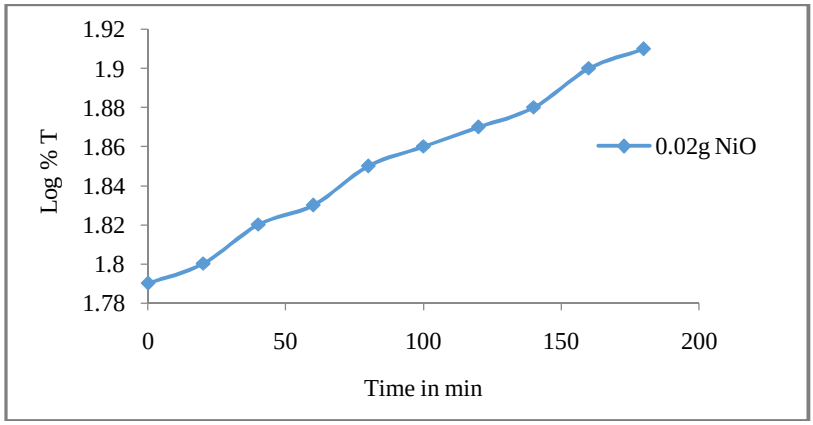

Figure 9. Plot of log % T Vs time with respect to re-use of catalyst.

CONCLUSION

With growing concerns over increasing pollution and waste production in the environment, we all have a responsibility to protect forests, water resources and environment. Green chemistry is the general practice across all the domains and fields of chemistry of reducing the use of chemical compounds in synthesis and processes at both research and industrial level. Hence the significance of isolating useful organic compounds from plant extracts has grown tremendously during the recent years. Biosynthesis of nanomaterials has been proposed as a cost effective and eco-friendly alternative to physical and chemical methods. Plant mediated synthesis of nanoparticles is a green chemistry approach that connects nanotechnology with plants.

In current work, nickel oxide nanoparticles have been synthesized by a green method under ambient temperature using *Acalypha Indica* leaf extract and nickel sulphate. The characterization techniques like XRD, FT-IR, FE-SEM, EDAX and UV-Visible are employed to identify the synthesized nanoparticles sample. The optical behavior is confirmed by UV Visible spectroscopy. The FT-IR characteristic bands revealed the functional group determination. The average crystallite size determined from XRD is 68.3nm with FCC structure. The photocatalytic activity outcomes have revealed that NiO nanoparticles could be as a photocatalyst for the degradation of indigo carmine under UV radiation.

ACKNOWLEDGEMENT

This research work has been supported by University of Mysore, Mysuru and the authors acknowledges UPE, CPEPA and DST Purse project, Vijnan Bhavan, University of Mysore for necessary instrumentation facilities. The authors are thankful to UGC-BSR, New Delhi for financial support.

REFERENCES

[1]. M. L. Peterson, A. F. White, G. E. Brown, G. A. Parks, Surface passivation of magnetite by reaction with aqueous Cr (VI): XAFS and TEM results, *Environ. Sci. Technol.*, **1997**, 31(5), 1573-1576.
[2]. D. K. Tiwari, Time and dose dependent antimicrobial potential of Ag nanoparticles synthesized by top-down approach, *Curr. Sci*., **2008**, 95, 647–655.
[3]. W. Wei, X. Jiang, L. Lu, X. Yang, X. Wang, Study on the catalytic effect of NiO nanoparticles on the thermal decomposition of TEGDN/NC propellant, *J. Hazard. Mater.*, **2009**, 168, 838-842.

[4]. Zahra Sabouri, Alireza Akbari, Hasan Ali Hosseini, Alireza Hashemzadeh, Majid Darroudi, Eco-friendly biosynthesis of nickel oxide nanoparticles mediated by okra plant extract and investigation of their photocatalytic, magnetic, cytotoxicity and antibacterial properties, *Journalof cluster science, Springer*, **2019**, 1-10, https://doi.org/10.1007/s10876-019-01584-x.
[5]. C. N. R. Rao, Chemical applications of infrared spectroscopy, Academic press, New York-London, **1963**.
[6]. C. N. R. Rao, Chemical approaches to the Synthesis of inorganic materials, New Delhi, Wiley Eastern Ltd, **1994**.
[7]. K. J. Rao, P. D. Ramesh, Use of microwaves for the synthesis and processing of materials, *Bull. Mater. Sci.*, **1995**, 18(4), 447-465.
[8]. G. V. Reddy Gopal, Sheela Kalyana, S. V.Manorama, *Int. J. Inorg. Mater*, **2000**, 2, 301.
[9]. J.Smith, H. P. J. Wijn, N. N. Phillips, G. Eindhoven Ferrites (Holland), **1959**, 144A.
[10]. D. A. Sverjensky, Physical surface complexation models for sorption at the mineral-water interface, *Nature*, **2003**, 364, 776-780.
[11]. N. N. Mallikarjuna, A. Venkataraman, Adsorption of $Pb2^{+}$ ions on nanosized γ-Fe_2O_3: formation of surface ternary complexes on ligand complexation, *Talanta*, **2003**, 60(1), 139-147.
[12]. N. N. Mallikarjuna, B. Govindraj, L. Arunkumar, A. Venkataraman, Combustion derived ultrafine γ-Fe_2O_3 structure, morphology and thermal studies, *Journal of thermal analysis and calorimetry*, **2003**, 71(3), 915-926.
[13]. J. C. Mallinson, The foundations of magnetic recording (San Diego: Academic press), **1987**.
[14]. A.Venkataraman, V. A. Hiremath, S. K. Date, S. M. Kulkarni, A new combustion route to γ-Fe_2O_3 synthesis, *Bull. Mater. Sci.*, **2001**, 24(6), 617-621.
[15]. S. V. Ganachari, R. Bhat. R. Deshpande, A. Venkataraman, Synthesis and characterization of nickel oxide nanoparticles by self propagating low temperature combustion method, *Recent research in science and Technology*, **2012**, 4(4), 50-53.
[16]. Murugan Perachiselvi, J. Jensonsamraj Muthiahsakthi Bagavathy, Thambiraj Arthi Feiona, Pitchumani Krishnaveni, E. Pushpa Lakshmi, V. Swetha, M. MargreetLeema, S. John Britto, G. Annadurai, Fabrication of nickel oxide nanoparticles for antibacterial and photocatalytic activity, *Research journal of life sciences, bioinfromatics, pharmaceutical and chemical sciences*, **2018**, DOI: 10.26479/2018.0406.59.
[17]. B. Nagaraj, N. B. Krishnamurthy, P. Liny, T. K. Divya, R. Dinesh, Biosynthesis of gold nanoparticles of Ixora coccinea flower extract & their antimicrobial activities, *International Journal of Pharma and Bio Sciences*, **2011**, 2(4), 557–565.
[18]. Muhammad Imran Din, Aneela Rani, Recent advances in the synthesis and stabilization of nickel oxide nanoparticles: a green adeptness, *International journal of analytical chemistry*, **2016**, Article ID: 3512145.
[19]. R. C. Monica, R. Cremonini, Nanoparticles and higher plants, *Caryologia*, **2009**, 62(2), 161–165.
[20]. A. Ahmad, P. Mukherjee, S. Senapati, Extracellular biosynthesis of silver nanoparticles using the fungus Fusarium oxysporum, *Colloids and Surfaces B: Biointerfaces*, **2003**, 28, 4, 313–318.
[21]. S. Sudhasree, A. Shakila Banu, P. Brindha, G. A. Kurian, Synthesis of nickel nanoparticles by chemical and green route and their comparison in respect to biological effect and toxicity, *Toxicological and Environmental Chemistry*, **2014**, 96(5), 743–754.
[22]. Aliakbar Dehno Khalaji, Debasis Das, Synthesis and characterization of NiO nanoparticles via solid-state thermal decomposition of nickel (II) Schiff base complexes, *Int. Nano.Lett.*, **2014**, 4, 117, DOI 10.1007/s40089-014-0117-4.
[23]. P. Karpagavinayagam, C. Vedhi, Green synthesis of NiO nanoparticles using mangroves and its electrochemical characterization, *International journal of science, engineering and management*, **2018**, 3(4), 699-702.
[24]. Chengfang Li, Gongwu Song, Photocatalytic degradation of organic pollutants and detection of chemical oxygen demand fluorescence method, *Sensors and Actuators B: Chemical*, **2009**, 137(2), 432-436.

[25]. G. Chaitanya Lakshmi, S. Ananda, R. Somashekar, C. Ranganathiah, Synthesis, characterization and photocatalyticactivity of ZnO:Sn nanocomposites, *International Journal of Advances Science and Technology*, **2012**, 5, 54-64.
[26]. M. A. Bhosale, B. M. Bhanage, Rapid synthesis of nickel oxide nanorods and its applications in catalysis, *Advanced powder technology*, **2015**, 26(2), 422–427.
[27]. A. K. Subramani, K. Byrappa, S. Ananda, K. M. Lokanatha Rai, C. Ranganathaiah, M. Yashimura, Photocatalytic degradation of Indigo Carmine dye using TiO_2 impregnated activated carbon, *Bulletin of Materials Science*, **2007**, 30(1), 37- 41.
[28]. Nesic Jelena., Manojlovic Dragan D, Andelkovic Ivan, Dojcinovic, P. Biljana, J. VulicPredrag, Krstic Jugoslav, M. Roglic Goran, Preparation, characterization and photocatalytic activity of Lanthanum and Vanadium Co-doped mesoporous TiO_2 for Azo-Dye degradation, *Journal of Molecular Catalysis A: Chemical*, **2013**, 378, 67-75.
[29]. Wenjuan Li, Danzhen Li, Jinxiu Wang, Yu Shao, JinmaoYou, Fei Teng, Exploration of the active species in thephotocatalytic degradation of Methyl Orange under UV light irradiation, *Journal of Molecular Catalysis A: Chemical*, **2013**, 380, 10-17.
[30]. K. R. Raksha, Sannaiah Ananda, An investigation on: kinetics of photo catalysis, electrical property and biological activity of electrochemically synthesized ZnS and Ru:ZnS nano photocatalysts, *J. Applicable Chem.*, **2014**, 3(1), 397- 412.